

## Article

# Effects of Dipentaerythritol and Cellulose as Additives on the Morphology of Pentaerythritol Crystals

Wang Wei <sup>1,†</sup>, Yangguang Li <sup>2,†</sup>, Ningning Tian <sup>2</sup>, Tian Xie <sup>1,3,4,5</sup>, Dengpan Nie <sup>1</sup>, Hongyan Li <sup>4,5</sup>, Hongdong Quan <sup>4,5</sup>, Xiuguo Yang <sup>4,5</sup>, Luqian Ye <sup>4,5</sup>, Xiaohe Li <sup>4,5</sup>, Kangli Li <sup>2,6,\*</sup> and Ye Gao <sup>6,\*</sup>

<sup>1</sup> School of Chemical Engineering, Guizhou Minzu University, Guiyang 550025, China; weiwang0720@126.com (W.W.); chemostar@163.com (T.X.); ndpz@sina.com (D.N.)

<sup>2</sup> State Key Laboratory of Chemical Engineering, School of Chemical Engineering and Technology, Tianjin University, Tianjin 300072, China; yangguangli@tju.edu.cn (Y.L.); tanningning@tju.edu.cn (N.T.)

<sup>3</sup> State Key Laboratory of Efficient Utilization for Low Grade Phosphate Rock and Its Associated Resource, Guiyang 550016, China

<sup>4</sup> Chifeng Ruiyang Chemical Co., Ltd., Chifeng 024000, China; lhy6699517@sina.com (H.L.); qhd6699517@sina.com (H.Q.); 13885018320@163.com (X.Y.); yeluqian1234@126.com (L.Y.); ilovexiaohe001@sohu.com (X.L.)

<sup>5</sup> Inner Mongolia Key Laboratory of Polyol Chemical New Material Enterprise, Chifeng 024000, China

<sup>6</sup> Institute of Shaoxing, Tianjin University, Shaoxing 312300, China

\* Correspondence: kangli\_li@163.com (K.L.); gaoye@tju.edu.cn (Y.G.)

† These authors contributed equally to this work.

**Abstract:** The crystal habit of pentaerythritol (PE) crystals is usually rod-shaped, which may lead to low bulk density and bad flowability compared with low aspect ratio crystals. In this study, dipentaerythritol (DPE), methylcellulose (MC), and hydroxypropyl methylcellulose (HPMC) were selected as additives to modify the morphology of PE crystals. In the presence of DPE, the bulk density of PE crystals was improved, and the aspect ratio was decreased. The modified attachment energy (AE) model was conducted to analyze changes in PE crystal habits in the presence of DPE, which characterizes the intensity of the interaction between DPE molecules and PE crystal faces. Spherical pentaerythritol crystals can be successfully prepared by adding MC and HPMC solution, and the formation mechanism can be divided into five steps.

**Keywords:** crystallization; additives; crystal morphology; pentaerythritol



**Citation:** Wei, W.; Li, Y.; Tian, N.; Xie, T.; Nie, D.; Li, H.; Quan, H.; Yang, X.; Ye, L.; Li, X.; et al. Effects of Dipentaerythritol and Cellulose as Additives on the Morphology of Pentaerythritol Crystals. *Crystals* **2024**, *14*, 219. <https://doi.org/10.3390/cryst14030219>

Academic Editor: Tom Leyssens

Received: 16 January 2024

Revised: 16 February 2024

Accepted: 20 February 2024

Published: 24 February 2024



**Copyright:** © 2024 by the authors. Licensee MDPI, Basel, Switzerland. This article is an open access article distributed under the terms and conditions of the Creative Commons Attribution (CC BY) license (<https://creativecommons.org/licenses/by/4.0/>).

## 1. Introduction

Crystallization is a vital step in the manufacture of pharmaceuticals and fine chemicals [1]. In the crystallization process, controlling particle attributes, such as the morphology of crystals, is important for the function and physical properties of a material. There are different factors that influence the morphology, like temperature [2], stirring rate, seed crystal [3], impurities [4], additives, and so on, among which the additives have attracted wide attention because of their simplicity, effectiveness, and low cost [5]. A great number of studies have shown that additives have an influence on the morphology [6–10] or growth rate of crystals. For example, specific additives may change the growth rate of different crystal faces [11]. Bellucci et al. found out that both methanol and polyvinylpyrrolidone (PVP) have a strong affinity for the (0 2 0) face of metformin hydrochloride, destabilizing it for growth (virtual face), which can result in needle-like habits, comprised the (1 0 0) and (1 1 0) faces [12].

Cellulose derivative additives are favored by researchers due to their advantages, such as high safety, low price, sources, and the obvious effect on crystals [13]. Different crystals, growing under cellulose systems, have been studied in the past decade. In 2009, HPMC was selected as one of the research objects to study the effect on the habit of hydrate crystals [14]. In 2012, HPMC proved to be effective in reducing both the nucleation and the growth

rates of felodipine crystals from supersaturated solutions [15]. After two years, Reis et al. reported that HPMC could slow the rate of generation of cloudiness in a paracetamol aqueous solution, which leads to the direct production of micronized Paracetamol crystals from the solution [16]. Since then, different research has been conducted to control the morphology of crystals by adding HPMC or other cellulose derivative additives [17–19].

Pentaerythritol (PE) crystal is an organic chemical product, produced by the reaction of formaldehyde and acetaldehyde under the action of an alkaline catalyst [20], and it is often crystallized through evaporation crystallization or cooling crystallization. The PE products are widely used in the fields of resins, coatings, chemicals, pharmaceuticals, and national defense. Several studies have been conducted to optimize the properties of PE crystals. In 1995, Chianese et al. measured the crystallization kinetics of pentaerythritol with different purities and used formaldehyde and formic acid as additives to explore their effects on the crystallization behavior of PE crystallization. They found that the presence of impurities in the crystal products can increase the solubility of pentaerythritol, and the nucleation growth rates of different purity crystals are significantly different [21,22]. In 2012, Kardum et al. studied the influence of crystallization process parameters on PE product properties by designing a single variable experiment [15]. After 2017, the application potential of energy storage in the solid–solid transition process of pentaerythritol has been noted by Venkitara et al., and recently, the team found that the thermochemical stability of PE will be significantly enhanced by using  $\text{Al}_2\text{O}_3$  as additives [23–25]. In industrial crystallization, the mother liquor of PE often consists of dipentaerythritol (DPE) and other impurities. For example, the mother liquor, named “Grade90”, consists of 63% pentaerythritol; other ingredients can be seen in Table 1. “Grade90” represents the mother liquid, and it can lead to products containing 90% mass fraction PE crystals. So are the Grade98 and Grade99. It is necessary to study the effect of DPE on the pentaerythritol crystals as different mother liquor can cause differences in morphology, granularity, bulk density, or even impurity.

**Table 1.** Mass composition of Grade90 and Grade98 PE mother liquor.

Name	SF	PE	DPE	Acetal	TPE	PPE	Other
Grade90	19	63	5	7	0.5	1	4.5
Grade98	26	36	14	5	1	3	15

Where SF represents sodium formate; PE represents pentaerythritol; DPE represents dipentaerythritol; TPE represents Tripentaerythritol; and PPE represents poly-pentaerythritol.

In this study, PE crystallization under the system of DPE and its comparison with the morphology of industrial products are reported. The attachment energy (AE) model is a tool to calculate the energy in the process of crystal growing, reflecting the growth rate of different crystal faces. Meanwhile, to correct the interaction between PE crystals and the solvent, the modified AE model is conducted to find out the influence of DPE on PE crystals. We also report the effect of the additives methylcellulose (MC) and hydroxypropyl methylcellulose (HPMC) on the morphology of PE crystallization and reveal the mechanism of the formation process of PE spherulites under the cellulose system.

## 2. Experiment Section

### 2.1. Materials and Instruments

Pentaerythritol was purchased from Shanghai Titan Scientific Co., Ltd., Shanghai, China with a purity of >98%. Dipentaerythritol was purchased from Shanghai Macklin Biochemical Co., Ltd., Shanghai, China with a purity of >90%, and was used through twice purification. Grade90 and Grade98 crystallization mother liquor were provided by Chifeng Ruiyang Chemical Co., Ltd., Inner Mongolia, China. Methanol, ethanol, isopropanol, and acetonitrile were purchased from Tianjin Kermel Chemical Reagent Co., Ltd., Tianjin, China, with a purity of >99.5%. Methylcellulose and hydroxypropyl methylcellulose were purchased from Shanghai Aladdin Biochemical Technology Co., Ltd, Shanghai, China.

The experiment was carried out in a jacketed crystallizer combined with a CF41 homogeneous program-controlled thermostatic bath (Julabo, Beijing, China) and condensing system. An OHS.1D overhead mechanical stirrer (Julabo, Beijing, China) and a BT100-1F precision peristaltic pump (Baoding Longer Precision Pump Co., Ltd., Baoding, China) were used for controlling the stirring and feeding rate, respectively. A 101-2AB blast drying oven (Tianjin Taisote Medical Equipment Inc., Tianjin, China) was used to dry the sample for characterization. A BX53 fluorescence microscope (OLYMPUS, Tokyo, Japan) and TM3000 scanning electron microscope (Hitachi, Japan) were used to observe the morphology of the crystals.

### 2.2. Preparation of Monodisperse Crystal Seeds

This experiment was carried out with the method of mixed solvent cooling crystallization; methanol, ethanol, isopropyl alcohol, and acetonitrile were selected as the undesirable solvents for a 50 °C saturated solution with a molar fraction of 0.4. The crystal products were cooled linearly to 10 °C at a rate of 10 °C/h. After rapid suction filtration and drying, it was characterized using a scanning electron microscope (SEM).

### 2.3. Growth Experiment of Pentaerythritol in the Presence of Additives

The single crystal growth process in the presence of dipentaerythritol (DPE) and its effect on the crystalline shape was explored. The experimental process of single-crystal cultivation of pentaerythritol started by preparing the saturated solution of each system at 25 °C according to the solubility data, which were measured before, and then the crystallization process was achieved with the help of solvent volatilization with fluorescence microscopy, used for regular observation. Finally, the simulation of crystal morphology was realized using a modified AE model in Materials Studio 6.5 software. During the calculation process, the thickness of the cut crystal face was  $3d_{hkl}$ , and it was expanded to a  $6 \times 6$  supercell structure to ensure that its size was greater than 2 times the truncation radius. The solvent layer was constructed in the Amorphous Cell module, with a set number of 500 water molecules and 10 DPE molecules added to imitate the real growth environment. The overall size of the solvent layer was the same as that of the crystal layer. During the combination process, a 50 Å vacuum layer was set on the upper layer of solvent molecules to eliminate free boundary interference. During the dynamic simulation process, the position of the crystal layer was fixed, and only the solvent layer molecules were allowed to move freely, with a step size of 1 fs and a total simulation time of 200 ps. The system temperature was controlled by an Andersen hot bath.

During the experiment of adding cellulose with different viscosities, the aqueous solution with MC or HPMC was first dissolved at a high temperature under stirring. After the solution was cleaned up, pentaerythritol (PE) was added and the temperature rapidly increased to 5 °C above the saturation temperature to ensure complete dissolution of PE. The product was filtered and dried at the end of the experiment after the system cooled down through the programmed linear cooling and analyzed by using a scanning electron microscope for characterization. At the same time, the time point of nucleation of pentaerythritol was determined at different MC additions, and the trend of the total number of particles in the solution was analyzed with the help of the pixact crystallization monitoring (PCM) online crystallization monitoring system.

### 2.4. AE Model

In the attachment energy (AE) model, the attachment energy  $E_{att}$  is expressed as the energy released by the growth of a layer of crystals on the crystal surface and its absolute value is positively correlated with the growth rate of the crystal surface. The smaller the  $E_{att}$  is, the slower the growth rate of the crystal surface [26,27]. In the real solution environment, the interaction between solvent molecules and the crystal surface cannot be neglected, and when the solvent molecules, adsorbed on the crystal surface, are removed, it will consume the system energy and further lead to a decrease in attachment energy. Therefore, the

modified AE model introduces the  $E_s$  term to characterize the effect of the solvent on the crystal growth process, the value of which can be calculated using the following equations:

$$E'_{\text{att}} = E_{\text{att}} - E_s \quad (1)$$

$$E_s = E_{\text{int}} \times A_{\text{acc}}/A_{\text{box}} \quad (2)$$

$$E_{\text{int}} = E_{\text{tot}} - E_{\text{sur}} - E_{\text{sol}} \quad (3)$$

$$S = A_{\text{acc}}/A_{\text{box}} \quad (4)$$

where  $E_s$  is the solvent correction term;  $A_{\text{box}}$  is the area of the crystalline surface;  $A_{\text{acc}}$  is the accessible area of the solvent on the corresponding crystalline surface, which can be calculated from the Connolly surface;  $E_{\text{tot}}$  represents the total energy of the solvent layer and the crystalline surface;  $E_{\text{sur}}$  and  $E_{\text{sol}}$  represent the energies of the crystalline surface and the solvent layer alone, respectively;  $E_{\text{int}}$  is the solvent-crystalline surface interaction energy; and  $S$  is the crystal surface roughness.

### 3. Results and Discussion

#### 3.1. Effect of Solvent on the Crystal Habit of Pentaerythritol

The method of cooling crystallization with mixed solvent was adopted and the results are shown in Figure 1. It can be seen that the morphology of the crystal products, except the isopropyl alcohol system, still conforms to the unique tetragonal dipyramidal crystal habit of pentaerythritol.

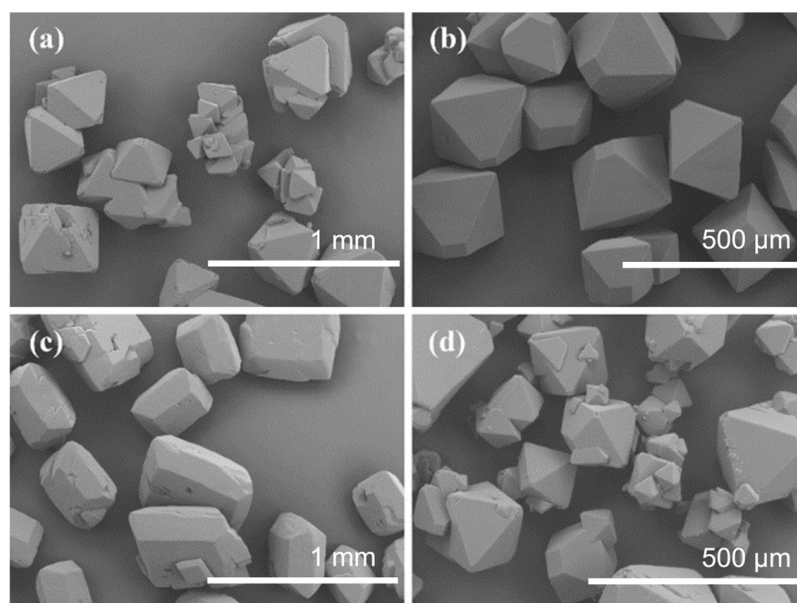


**Figure 1.** Comparison of the crystal morphology of pentaerythritol, obtained by cooling crystallization in the mixed solvents: (a) methanol; (b) ethanol; (c) isopropanol; and (d) acetonitrile.

Compared with other systems, like methanol, isopropanol, and acetonitrile, the ethanol system (Figure 1b) provides a great method to prepare pentaerythritol monodisperse crystal seeds and the crystal products are basically all single crystals with smooth crystal surfaces. Meanwhile, there are no twins or agglomerated crystals, which can reach the expected optimization goal and provide high-quality crystal seeds to control the crystallization process.



### 3.2. Effect of Dipentaerythritol on Crystal Habit of Pentaerythritol

#### 3.2.1. Effect of Dipentaerythritol on the Morphology of Pentaerythritol

For the pentaerythritol system, the crystal morphology varies greatly with the composition of the raw material. As is shown in Figure 2, the product made from Grade90 is long and rod-like. Its aspect ratio is about 3~5, and the bulk density is only  $0.63 \text{ g/cm}^3$ . While the product made from Grade98 is block-like, and the bulk density can reach  $0.82 \text{ g/cm}^3$ .

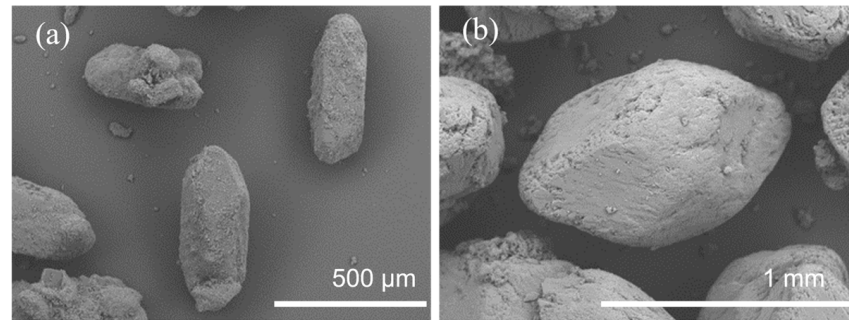


**Figure 2.** SEM images of PE products. (a) Grade 90 and (b) Grade98.

Therefore, the effect of dipentaerythritol (DPE) on PE crystal morphology was studied. The result is shown in Figure 3b.

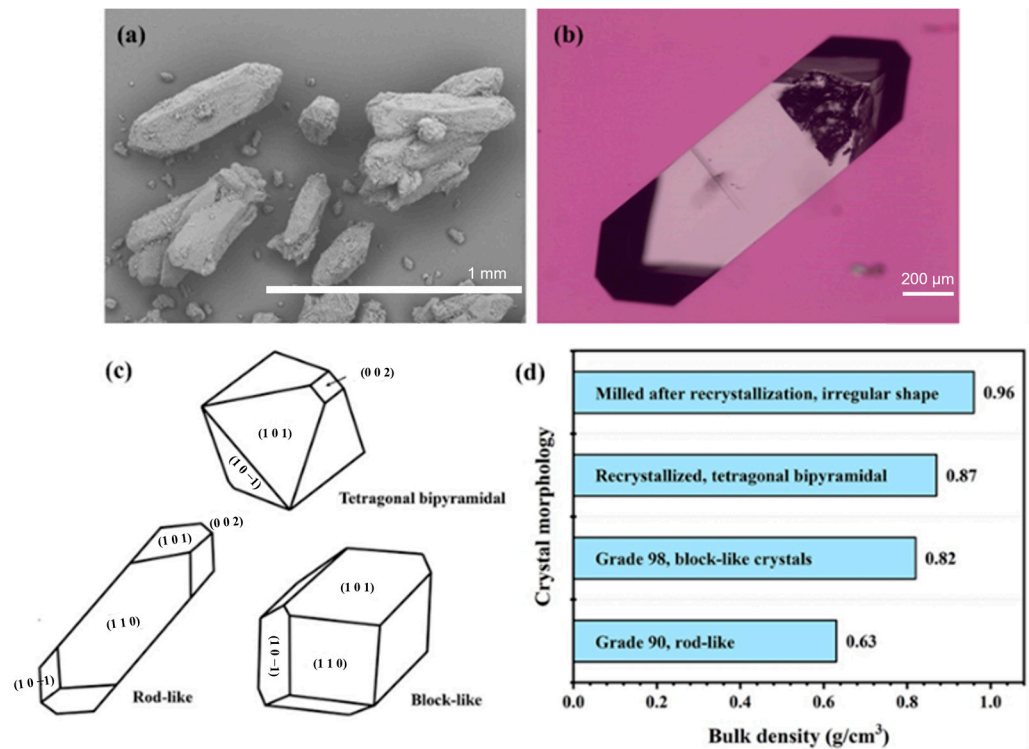


**Figure 3.** Comparison of the crystal morphology and corresponding bulk density of pentaerythritol in the presence of DPE additives. (a) SEM image of PE products made from Grade 90; (b) SEM image of single PE crystal in the presence of DPE; (c) morphological diagram of PE crystal; and (d) crystal morphology and bulk density diagram of different products.

It can be found that the morphology of the single PE crystal in the presence of DPE is the same as that of PE products made from Grade90 and both of the crystals grow in a symmetrical tetragonal bipyramidal column, with the crystal face (1 1 0) occupying the largest area proportion. With the decrease in the DPE content in the crystalline raw material liquid, the aspect ratio of the corresponding crystal product also gradually decreases, and

the crystal finally presents a perfect tetragonal bipyramidal shape with an aspect ratio of about 1. Therefore, it can be determined that the DPE is the key factor that affects the crystal habit of PE, and the selective growth inhibition of PE crystal faces is the main reason for the increase in the aspect ratio of crystal products.

### 3.2.2. Analysis of Crystal Surface Parameters and Crystal Habit Simulation Results

The molecular dynamics simulation can directly reflect the state of solute molecules on the crystal surface and the interaction energy between the crystal surface and solvent during crystal growth, which contributes to analyzing the influence mechanism of DPE on the growth of PE crystals. Thus, based on the foregoing experimental phenomena, the Morphology module in the Materials Studio 6.5 software (MS software) was used to calculate the morphology and crystal surface parameters of pentaerythritol in the AE model in a vacuum state. The results are shown in Table 2.

**Table 2.** Crystal surface parameters of pentaerythritol under vacuum conditions.

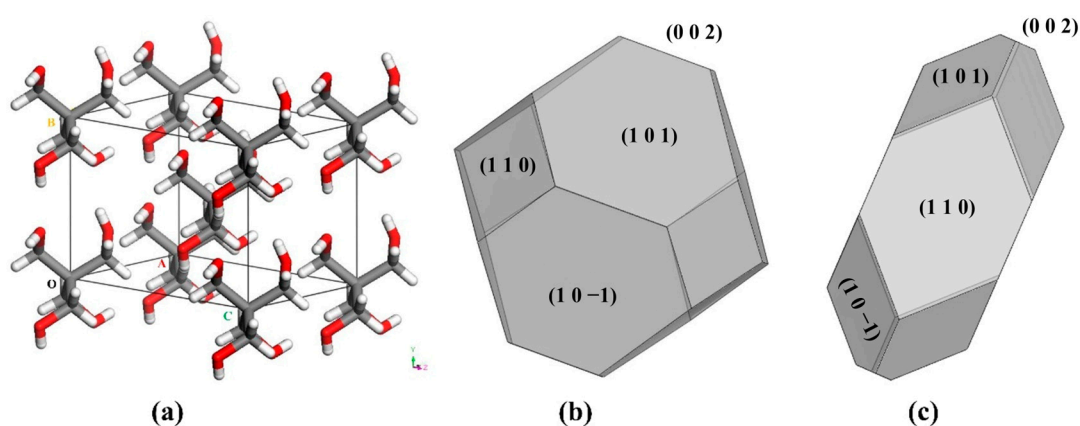
Crystal Face ( <i>h k l</i> )	Dimension	$A_{\text{box}}$	$E_{\text{att}}$	Crystal Surface Proportion %
(1 0 1)	4	32.51	−35.97	40.40
(1 0 −1)	4	32.51	−35.97	40.40
(0 0 2)	2	37.00	−41.47	7.68
(1 1 0)	4	37.81	−43.63	11.52

The simulation results show that there are four main crystal faces of pentaerythritol, with (1 0 1) and (1 0 −1) crystal faces, accounting for the largest proportion, each of which is about 40.4%; (0 0 2) crystal faces have the dimension of 2, with a total proportion of 7.68%; and (1 1 0) crystal faces account for 11.52%. According to the AE model, the proportion of each crystal face is inversely proportional to its growth rate, meaning that the faster the growth rate of the crystal face is, the smaller its proportion is. Furthermore, the growth rate of each crystal face is essentially determined by the arrangement of solute molecules inside it and is affected by external factors, such as supersaturation, impurities, temperature, and solvents [28–31].

Table 3 gives the parameters of each crystal surface of pentaerythritol in the modified AE model under the condition that the solvent layer has been added with dipentaerythritol molecules. The modified crystal habit, calculated from this, is shown in Figure 4. Point A, B and C represent the vertex of cubic crystal cell. It can be seen that the crystal habits, obtained from molecular simulation, are the same as the results of single-crystal incubation experiments, and the only difference consists in the proportion of (1 1 0) crystal faces. It should be noted that  $E'_{\text{att}}$  is corrected according to the solvent action term  $E_s$ , which changes accordingly with the change of the DPE molecules in the solvent layer. This is in line with the phenomenon of the effect of DPE content on the crystal habit of PE in the actual crystallization process. By comparing the interaction energies with the solvent layer, it can be seen that there is a big difference between each crystal face except the (1 0 1) and (1 0 −1) crystal faces. The (1 1 0) crystal face has the strongest  $E_{\text{int}}$ , which is approximately 3 times that of the (0 0 2) crystal face. Corresponding to the interaction force, the value of the correction term  $E_{\text{att}}$  of (1 1 0) crystal face is also the largest. Therefore, when the original adhesion energy  $E_{\text{att}}$  of each crystal face is similar, the strong force of solvents and DPE molecules makes the growth rate of the crystal face decrease and the area proportion increase.

**Table 3.** The modified attachment parameters of PE crystal surfaces in the presence of DPE.

Crystal Face ( <i>h k l</i> )	$E_{tot}$	$E_{sur}$	$E_{sol}$	$E_{int}$
(1 0 1)	−6376.38	−2233.01	−3699.93	−443.44
(1 0 −1)	−6321.58	−2233.01	−3630.85	−457.72
(0 0 2)	−6379.10	−2546.13	−3570.30	−262.66
(1 1 0)	−6110.07	−1832.11	−3508.26	−769.71
Crystal Face ( <i>h k l</i> )	$A_{acc}$	$S$	$E_s$	$E'_{att}$
(1 0 1)	40.33	1.24	−15.28	−20.69
(1 0 −1)	40.31	1.24	−15.76	−20.21
(0 0 2)	45.84	1.24	−9.04	−32.43
(1 1 0)	52.74	1.39	−29.82	−13.81

**Figure 4.** The cell structure and simulated crystal morphology of pentaerythritol in the aqueous solution of DPE; (a) unit cell structure; (b) crystal morphology under vacuum condition; and (c) modified morphology in the presence of DPE.

### 3.2.3. Crystal Surface Roughness and Selective Adsorption of Dipentaerythritol Molecules

From Table 2, the adhesion energy  $E_{att}$  and the proportion of crystal faces of (1 0 1) and (1 0 −1) crystal faces are the same. However, the crystal habits of the two crystal faces are not completely symmetric, and the area of the former is relatively large as shown in Figure 3c. To further explore the differences in the solute molecular arrangement of each crystal face, the crystal-solvent phase interface of pentaerythritol in aqueous solution was cut in the experiment, as shown in Figure 5, in which the pink dot represents the surface where solvent action can reach.

Corresponding to the crystal face parameters in Table 2, it shows that the solute molecular arrangement of the crystal face (1 0 1) and (1 0 −1) is highly similar, and the surface functional groups are both hydroxymethyl and hydroxyl, which explains why the crystal face parameters are identical in a vacuum. While in the actual crystallization environment, there are still slight differences in the crystal face-solvent interaction between the two crystal faces due to the difference in the arrangement of solute molecules. The  $E_{int}$  values in Table 3 are 443.44 kcal/mol and 457.72 kcal/mol, which also results in asymmetric crystal habits, as shown in Figure 4c. For the (0 0 2) crystal face, the chemical functional group on its surface is only methene, which is difficult to chemically interact with solvents or DPE molecules and is less affected by the solvent layer, determining that the correction term  $E_s$  of it is only 9.04 kcal/mol. On the contrary, the functional group of the (1 1 0) crystal face is dominated by the overstretched hydroxyl group, which makes it easy to form the hydrogen bond interaction with the solvent layer, leading to high  $E_{int}$  and  $E_s$ . In addition, comparing the crystal surface roughness using Equation (4), the value of the (1 0 1), (1 0 −1), or (0 0 2) crystal face equals 1.24, but the value of (1 1 0) equals 1.39. That

means a relatively rough crystal face can provide more surface area to contact the solvent layer, and its larger solute molecular spacing can better match the large volume of DPE molecules in space; thus, forming stronger hydrogen bonding and inhibiting crystal surface growth. The interaction energy between DPE molecules and each crystal face of PE was further calculated, and the results are shown in Figure 6.

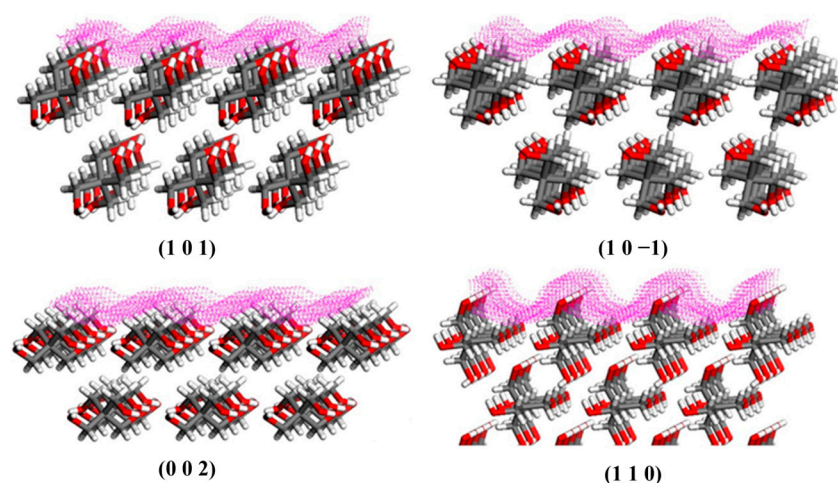


**Figure 5.** The schematic diagram of crystal surface-solvent interfaces of pentaerythritol in water.

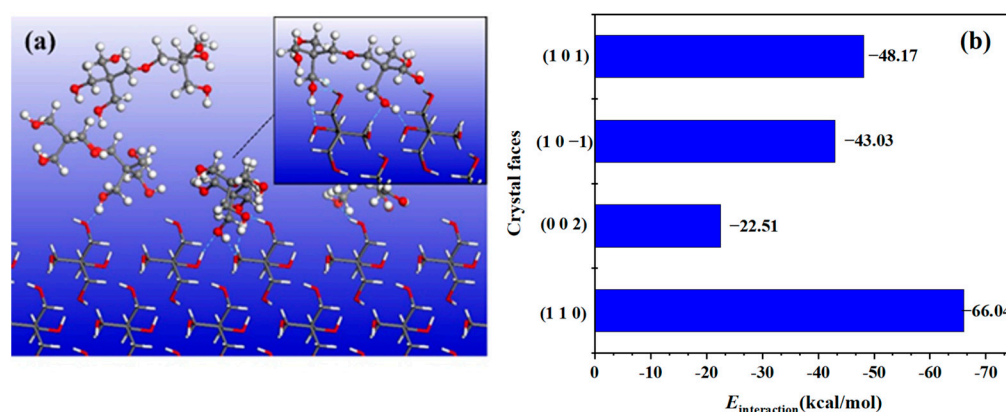


**Figure 6.** The selective adsorption of DPE molecules and the interaction energies between DPE and PE crystal surfaces. (a) Equilibrium adsorption conformation of the DPE molecules on (1 1 0) crystal face and (b) Interaction energy of 4 crystal faces.

Figure 6a shows that DPE molecules can be closely bonded by hydrogen bonding with a (1 1 0) crystal face, and the conformation of DPE molecules is also reversed under the action of the solute, leading to a better match to the crystal face structure. In Figure 6b, the interaction energy between DPE and all crystal faces of pentaerythritol is negative, indicating the existence of intermolecular force, and its absolute values are  $(1\ 1\ 0) > (1\ 0\ 1) > (1\ 0\ -1) > (0\ 0\ 2)$ . Meanwhile, the numerical difference in the adsorption energy of each crystal surface indicates that the adsorption of the DPE is selective. According to the values, the adsorption of the DPE molecules on the (1 1 0) crystal face is the strongest; thus, the DPE molecules occupy a certain number of growth sites, which prevents the growth unit from moving closer to the crystal. Finally, the crystal face is inhibited from growing, while the (0 0 2) crystal face is just the opposite. Comparing the (1 0 1) and (1 0 -1) crystal faces with similar conformation, since the adsorption energy of the former is slightly stronger, the growth rate reduces, leading to a larger area proportion. To conclude, the DPE molecules in the solution will affect the relative growth rate of each crystal face of pentaerythritol



mainly through selective adsorption, resulting in an increase in aspect ratio and a decrease in particle size.

### 3.3. Effect of Cellulose Species on the Crystal Habit of Pentaerythritol Crystals

#### 3.3.1. Effect of Cellulose Species on the Morphology of Pentaerythritol Crystals

From the previous section, it can be found that the single-crystal habit in the presence of DPE is also in the form of long rods, and the main factor to affect the crystal morphology is the DPE. Both PE and DPE are rich in hydroxyl functional groups, and the hydrogen bonding between them can interact with each other. Therefore, celluloses with higher hydroxyl content were selected for the study, including methylcellulose (MC) and hydroxypropyl methylcellulose (HPMC). The SEM photos of the PE crystals, obtained from the two cellulose systems with different viscosities at the same controlled additive amount of 0.3 wt.% are shown in Figure 7.

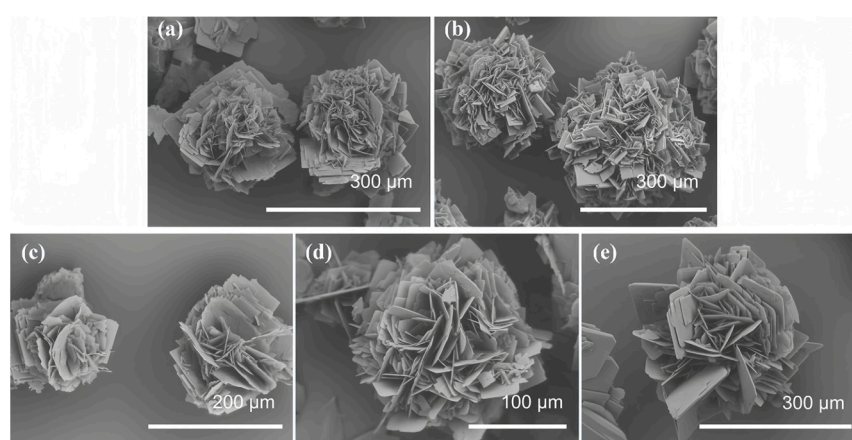


**Figure 7.** Crystal morphologies of pentaerythritol in different cellulose systems. (a) 15 mPa·s MC; (b) 1500 mPa·s MC; (c) 3 mPa·s HPMC; (d) 50 mPa·s HPMC; and (e) 100 mPa·s HPMC.

In Figure 7, it can be seen that both the PE crystals under cellulose systems consisted of square lamellar dendrites in a similar spherical shape. On the whole, the crystals with MC are denser than the HPMC system, and the crystal size is larger, up to 300  $\mu\text{m}$  in diameter, while the crystals in the HPMC system under the same conditions are only about 150–200  $\mu\text{m}$ .

In addition, under the action of the same additive, the crystal morphology in the high-viscosity system is relatively more uniform, and the degree of sphericity and density is higher. This phenomenon is particularly obvious under the action of MC, and the standard viscosity of the two additives is nearly 100 times different from each other. Therefore, in addition to the type of cellulose, the difference in its viscosity is also one of the important factors that affects the spherulite morphology.

#### 3.3.2. Effect of Cellulose Additive Amount on the Morphology of Pentaerythritol Crystals

The viscosities of 15 mPa·s MC and 50 mPa·s HPMC were selected to investigate the effect of cellulose additive amount on the morphology of pentaerythritol crystals, and the results are shown in Figures 8 and 9.

In Figure 8, it can be seen that the crystal morphology in the MC system has a greater magnitude of change. When the addition of MC reaches 0.75%, the size of the dendrites and gaps are the same, with completely symmetrical radial growth. However, in the same conditions of the HPMC system of the crystalline products, there are larger dendritic crystal size differences in the spherical surface of the relative roughness and the crystal surface gaps. Comparing the morphology of spherical crystals in the two cellulose systems, it can be seen that under the same conditions, the increase in the number of dendrites will rapidly consume the supersaturation of the crystalline system. Thus, the driving force of dendritic

crystal growth will reduce, and the crystals tend to be more well-distributed and denser. At the same time, this phenomenon also shows that the increase in cellulose concentration can induce enhanced crystal branching, which is more conducive to the formation of perfect spherical crystals.

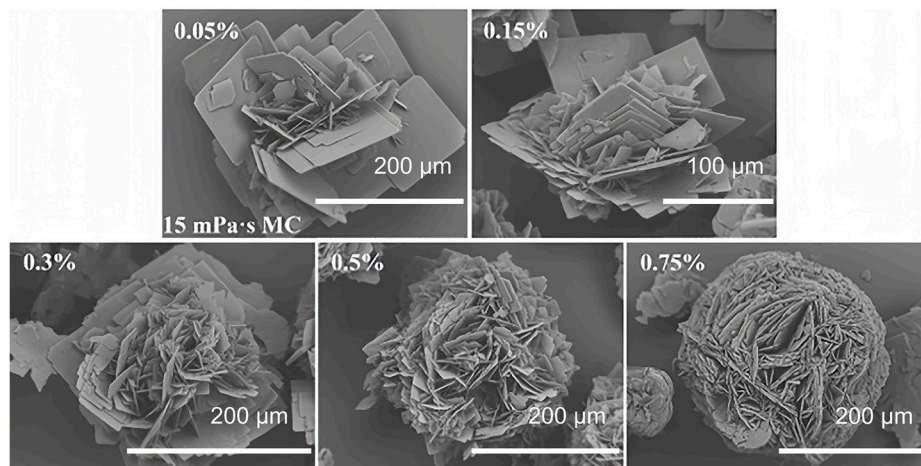


**Figure 8.** Crystal morphologies of pentaerythritol in the presence of different additive amounts of MC.

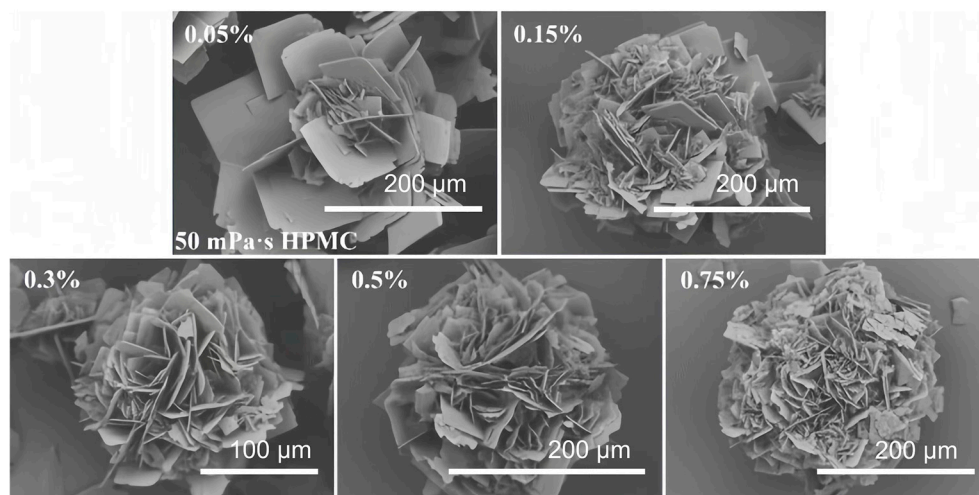


**Figure 9.** Crystal morphologies of pentaerythritol in the presence of different additive amounts of HPMC.

### 3.3.3. Analysis of the Mechanism of Cellulose Action

To investigate the formation mechanism of pentaerythritol spherical crystals, intermittent sampling was used to obtain the crystal products at different growth stages, and the SEM photos are shown in Figure 10.

According to the crystal morphology, the growth process is roughly divided into five stages: 1. spontaneous nucleation of solute molecules under the action of crystallization driving force and growth into lamellar crystals; 2. non-crystallographic branching of mother crystals, induced by cellulose and formation of polycrystals; 3. polycrystalline agglomerates growing in the supersaturated state, and at the same time due to the action of additives, branching taking place in the newly formed dendrite crystals; 4. the peripheral dendrites growth and branching occurring simultaneously, and the peripheral dendrites arranged in spiral rows; thus, forming rosette crystals; and 5. the dendrites, formed by branching, gradually filling the polycrystalline interstices and forming dense spherical crystals. It should be noted that cellulose plays two main roles in this process: changing the crystal

habit of pentaerythritol and inducing non-crystallographic branches. There are significant differences in the intensity of the interaction force among crystal faces of PE and the cellulose hydroxyl functional group. At the same time, the presence of cellulose increases the viscosity of the crystalline solution, and changes in the diffusion rate of solute molecules should also be taken into account.

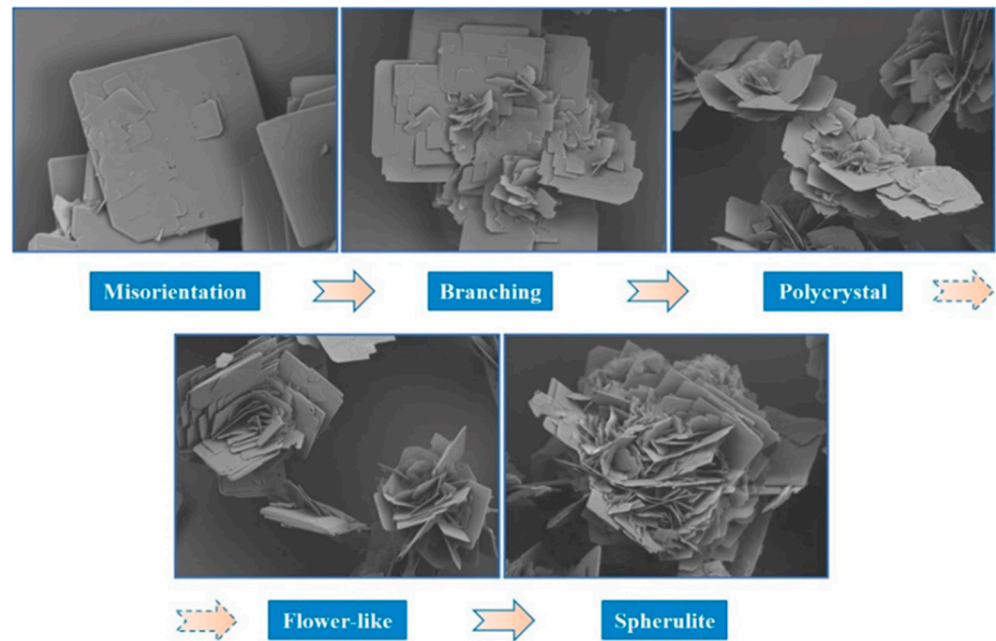


**Figure 10.** Illustration of the formation process of pentaerythritol spherulites obtained in the presence of cellulose additives.

Meanwhile, the nucleation time point of pentaerythritol with different additions of methylcellulose was experimentally determined. The results are shown in Figure 11.

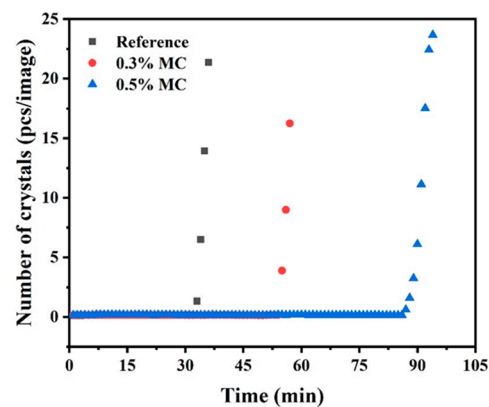


**Figure 11.** The variation trend of crystal counts under different MC additive amounts.

In Figure 11, it can be seen that the presence of cellulose in the solution can significantly inhibit the nucleation behavior of PE, and the degree of inhibition is positively correlated with the cellulose content. Therefore, the high supersaturation, accumulated during the crystallization process, will promote the occurrence of heterogeneous nucleation on the crystal surface and generate more branches, so that the spherulites will develop laterally along it. In contrast, the increase of spherulite particle size is achieved with the help of the radial growth of dendrites, in which the part near the outer edge preferentially grows. The dendrites in the center of the crystal lamellar are usually small in size and densely distributed, due to late formation time and the steric hindrance of solute diffusion.

#### 4. Conclusions

In conclusion, both DPE and cellulose (i.e., MC and HPMC) have a great effect on the morphology of PE crystals. The molecular dynamics simulation results show that the adsorption of DPE molecules on pentaerythritol crystal faces is selective, and the growth inhibition of the (1 1 0) crystal faces is the main reason for the change of pentaerythritol crystal habits, causing PE crystals to form a rod-like shape. The concentration of DPE in the mother liquor can be reduced for a lower aspect ratio and higher bulk density of PE crystal. Furthermore, Cellulose additives play two main roles in this process: changing the crystal habit of pentaerythritol and inducing amorphous branching. Their inhibition of the nucleation behavior of pentaerythritol will cause the accumulation of solution supersaturation, promote the occurrence of heterogeneous nucleation on the crystal surface, produce more branches, and finally form spherical crystals.

**Author Contributions:** Writing—original draft preparation, W.W., Y.L. and N.T.; illustration drawing, W.W. and N.T.; review and editing, T.X., D.N., H.L., H.Q., X.Y., L.Y., X.L., K.L. and Y.G. All authors have read and agreed to the published version of the manuscript.

**Funding:** This study was financially supported by the National Natural Science Foundation of China (22078234), and the Inner Mongolia Autonomous Region science and technology plan project (2023YFKL0008).

**Data Availability Statement:** The original contributions presented in the study are included in the article, further inquiries can be directed to the corresponding author.

**Acknowledgments:** We appreciate all authors and contributors for their hard work.

**Conflicts of Interest:** Author Tian Xie, Hongyan Li, Hongdong Quan, Xiuguo Yang, Luqian Ye and Xiaohe Li was employed by the company Chifeng Ruiyang Chemical Co., Ltd. The remaining authors declare that the research was conducted in the absence of any commercial or financial relationships that could be construed as a potential conflict of interest.

#### References

1. Yu, Z.Q.; Chew, J.W.; Chow, P.S.; Tan, R.B.H. Recent Advances in Crystallization control. *Chem. Eng. Res. Des.* **2007**, *85*, 893–905. [[CrossRef](#)]
2. Simone, E.; Klapwijk, A.R.; Wilson, C.C.; Nagy, Z.K. Investigation of the Evolution of Crystal Size and Shape during Temperature Cycling and in the Presence of a Polymeric Additive Using Combined Process Analytical Technologies. *Cryst. Growth Des.* **2017**, *17*, 1695–1706. [[CrossRef](#)]
3. Abbou Oucherif, K.; Raina, S.; Taylor, L.S.; Litster, J.D. Quantitative analysis of the inhibitory effect of HPMC on felodipine crystallization kinetics using population balance modeling. *CrystEngComm* **2013**, *15*, 2197–2205. [[CrossRef](#)]
4. Nordstrom, F.L.; Linehan, B.; Teerakapibal, R.; Li, H. Solubility-Limited Impurity Purge in Crystallization. *Cryst. Growth Des.* **2019**, *19*, 1336–1346. [[CrossRef](#)]
5. Tan, M.; Huang, X.; Song, W.; Wang, T.; Wang, N.; Bai, X.; Wang, Q.; Yu, H.; Zhou, L.; Hao, H. Uncovering the Coupling Mechanism of Enhanced Growth of Acephate by Additives: Experiments and Molecular Dynamics Simulations. *Cryst. Growth Des.* **2023**, *23*, 8426–8435. [[CrossRef](#)]
6. Yang, J.; Wang, Y.; Hao, H.; Xie, C.; Bao, Y.; Yin, Q.; Gong, J.; Jiang, C.; Hou, B.; Wang, Z. Spherulitic Crystallization of L-Tryptophan: Characterization, Growth Kinetics, and Mechanism. *Cryst. Growth Des.* **2015**, *15*, 5124–5132. [[CrossRef](#)]
7. Wang, G.; Li, L.; Lan, J.; Chen, L.; You, J. Biomimetic crystallization of calcium carbonate spherules controlled by hyperbranched polyglycerols. *J. Mater. Chem.* **2008**, *18*, 2789–2797. [[CrossRef](#)]
8. Vetter, T.; Mazzotti, M.; Brozio, J. Slowing the Growth Rate of Ibuprofen Crystals Using the Polymeric Additive Pluronic F127. *Cryst. Growth Des.* **2011**, *11*, 3813–3821. [[CrossRef](#)]
9. Klapwijk, A.R.; Simone, E.; Nagy, Z.K.; Wilson, C.C. Tuning Crystal Morphology of Succinic Acid Using a Polymer Additive. *Cryst. Growth Des.* **2016**, *16*, 4349–4359. [[CrossRef](#)]
10. Guo, X.; Yuan, J.; Ji, Z.; Su, M. Influences of additives on the crystal habit of potassium chloride. *Front. Chem. Eng. China* **2010**, *4*, 78–81. [[CrossRef](#)]
11. Hatcher, L.E.; Li, W.; Payne, P.; Benyahia, B.; Rielly, C.D.; Wilson, C.C. Tuning Morphology in Active Pharmaceutical Ingredients: Controlling the Crystal Habit of Lovastatin through Solvent Choice and Non-Size-Matched Polymer Additives. *Cryst. Growth Des.* **2020**, *20*, 5854–5862. [[CrossRef](#)]
12. Bellucci, M.A.; Marx, A.; Wang, B.; Fang, L.; Zhou, Y.; Greenwell, C.; Li, Z.; Becker, A.; Sun, G.; Brandenburg, J.G.; et al. Effect of Polymer Additives on the Crystal Habit of Metformin HCl. *Small Methods* **2023**, *7*, e2201692. [[CrossRef](#)]



13. Yu, S.; Wang, Z.; Ma, Y.; Xue, F. Effect of natural polymer additives on crystal form and morphology of clozapine anhydrate and monohydrate. *J. Mol. Liq.* **2022**, *364*, 119985. [[CrossRef](#)]
14. Tian, F.; Baldursdottir, S.; Rantanen, J. Effects of polymer additives on the crystallization of hydrates: A molecular-level modulation. *Mol. Pharm.* **2009**, *6*, 202–210. [[CrossRef](#)] [[PubMed](#)]
15. Sander, A.; Kardum, J.P. Pentaerythritol crystallization—Influence of the process conditions on the granulometric properties of crystals. *Adv. Powder Technol.* **2012**, *23*, 191–198. [[CrossRef](#)]
16. Reis, N.M.; Liu, Z.K.; Reis, C.M.; Mackley, M.R. Hydroxypropyl Methylcellulose as a Novel Tool for Isothermal Solution Crystallization of Micronized Paracetamol. *Cryst. Growth Des.* **2014**, *14*, 3191–3198. [[CrossRef](#)]
17. Chen, J.; Ormes, J.D.; Higgins, J.D.; Taylor, L.S. Impact of surfactants on the crystallization of aqueous suspensions of celecoxib amorphous solid dispersion spray dried particles. *Mol. Pharm.* **2015**, *12*, 533–541. [[CrossRef](#)] [[PubMed](#)]
18. Poornachary, S.K.; Chia, V.D.; Yani, Y.; Han, G.; Chow, P.S.; Tan, R.B.H. Anisotropic Crystal Growth Inhibition by Polymeric Additives: Impact on Modulation of Naproxen Crystal Shape and Size. *Cryst. Growth Des.* **2017**, *17*, 4844–4854. [[CrossRef](#)]
19. Simone, E.; Cenzato, M.V.; Nagy, Z.K. A study on the effect of the polymeric additive HPMC on morphology and polymorphism of ortho-aminobenzoic acid crystals. *J. Cryst. Growth* **2016**, *446*, 50–59. [[CrossRef](#)]
20. Bernardo, A.; Giulietti, M. Modeling of crystal growth and nucleation rates for pentaerythritol batch crystallization. *Chem. Eng. Res. Des.* **2010**, *88*, 1356–1364. [[CrossRef](#)]
21. Chianese, A.; Karel, M.; Mazzarotta, B. Crystal growth kinetics of pentaerythritol. *Chem. Eng. J. Biochem. Eng. J.* **1995**, *58*, 215–221. [[CrossRef](#)]
22. Chianese, A.; Karel, M.; Mazzarotta, B. Nucleation kinetics of pentaerythritol. *Chem. Eng. J. Biochem. Eng. J.* **1995**, *58*, 209–214. [[CrossRef](#)]
23. Venkitaraj, K.P.; Suresh, S.; Praveen, B.; Venugopal, A.; Nair, S.C. Pentaerythritol with alumina nano additives for thermal energy storage applications. *J. Energy Storage* **2017**, *13*, 359–377. [[CrossRef](#)]
24. Venkitaraj, K.P.; Suresh, S. Experimental thermal degradation analysis of pentaerythritol with alumina nano additives for thermal energy storage application. *J. Energy Storage* **2019**, *22*, 8–16. [[CrossRef](#)]
25. Venkitaraj, K.P.; Suresh, S. Effects of Al<sub>2</sub>O<sub>3</sub>, CuO and TiO<sub>2</sub> nanoparticles on thermal, phase transition and crystallization properties of solid-solid phase change material. *Mech. Mater.* **2019**, *128*, 64–88. [[CrossRef](#)]
26. Michael, B.; Sarah, L.P. Morphologies of Organic Crystals: Sensitivity of Attachment Energy Predictions to the Model Intermolecular Potential. *Crystal Growth Design* **2001**, *1*, 447–453. [[CrossRef](#)]
27. Tilbury, C.J.; Green, D.A.; Marshall, W.J.; Doherty, M.F. Predicting the Effect of Solvent on the Crystal Habit of Small Organic Molecules. *Cryst. Growth Des.* **2016**, *16*, 2590–2604. [[CrossRef](#)]
28. Constance, E.N.; Mohammed, M.; Mojibola, A.; Egiefameh, M.; Daodu, O.; Clement, T.; Ogundolie, T.; Nwawulu, C.; Aslan, K. Effect of Additives on the Crystal Morphology of Amino Acids: A Theoretical and Experimental Study. *J. Phys. Chem. C* **2016**, *120*, 14749–14757. [[CrossRef](#)]
29. Liang, Z.; Zhang, M.; Wu, F.; Chen, J.-F.; Xue, C.; Zhao, H. Supersaturation controlled morphology and aspect ratio changes of benzoic acid crystals. *Comput. Chem. Eng.* **2017**, *99*, 296–303. [[CrossRef](#)]
30. Ye, C.P.; Ding, X.X.; Li, W.Y.; Mu, H.; Wang, W.; Feng, J. Determination of crystalline thermodynamics and behavior of anthracene in different solvents. *AIChE J.* **2018**, *64*, 2160–2167. [[CrossRef](#)]
31. Han, D.; Wang, Y.; Yang, Y.; Gong, T.; Chen, Y.; Gong, J. Revealing the role of a surfactant in the nucleation and crystal growth of thiamine nitrate: Experiments and simulation studies. *CrystEngComm* **2019**, *21*, 3576–3585. [[CrossRef](#)]

**Disclaimer/Publisher’s Note:** The statements, opinions and data contained in all publications are solely those of the individual author(s) and contributor(s) and not of MDPI and/or the editor(s). MDPI and/or the editor(s) disclaim responsibility for any injury to people or property resulting from any ideas, methods, instructions or products referred to in the content.